



**HAL**  
open science

# The New Copper Composite of Pastes for Si Solar Cells Front Electrode Application

Piotr Panek, Robert Socha, Grzegorz Putynkowski, Abdelilah Slaoui

## ► To cite this version:

Piotr Panek, Robert Socha, Grzegorz Putynkowski, Abdelilah Slaoui. The New Copper Composite of Pastes for Si Solar Cells Front Electrode Application. *Energy Procedia*, 2016, 92, pp.962-970. <10.1016/j.egypro.2016.07.108>. <hal-05490435>

**HAL Id: hal-05490435**

**<https://univoak.hal.science/hal-05490435v1>**

Submitted on 3 Feb 2026

HAL is a multi-disciplinary open access archive for the deposit and dissemination of scientific research documents, whether they are published or not. The documents may come from teaching and research institutions in France or abroad, or from public or private research centers.

L'archive ouverte pluridisciplinaire HAL, est destinée au dépôt et à la diffusion de documents scientifiques de niveau recherche, publiés ou non, émanant des établissements d'enseignement et de recherche français ou étrangers, des laboratoires publics ou privés.



Distributed under a Creative Commons CC BY-NC-ND 4.0 - Attribution - Non-commercial use - No Derivative Works - International License



6th International Conference on Silicon Photovoltaics, SiliconPV 2016

## The new copper composite of pastes for Si solar cells front electrode application

Piotr Panek<sup>a\*</sup>, Robert P. Socha<sup>b</sup>, Grzegorz Putynkowski<sup>c</sup>, Abdelilah Slaoui<sup>d</sup>

<sup>a</sup>*Institute of Metallurgy and Materials Science PAS, Reymonta 25, 30-059 Krakow, Poland*

<sup>b</sup>*Institute of Catalysis and Surface Chemistry PAS, Niezapominajek 8, 30-239 Krakow, Poland*

<sup>c</sup>*Research and Development Center of Technology for Industry, Zlota 59, 00-120 Warsaw, Poland*

<sup>d</sup>*ICube, 23 rue du Loess, BP 20 CR, 67037 Strasbourg, France*

---

### Abstract

In this paper we present a new composite (CuXX) of pastes for formation electrodes in crystalline silicon solar cells. The CuXX composite is obtained by chemical processing of copper particles and added to commercially available paste used for front electrode deposition on Si solar cell. The CuXX offers a possibility to exchange over 50 wt. % Ag into Cu, which significantly decreases the material cost and therefore overall solar cell price. Solar cells with 50% wt. share of Cu as front electrode pastes were fabricated. The cells were characterized by current-voltage and spectral response techniques. Despite the non-optimized fabrication process, Cz-Si based solar cells with an efficiency approaching 14% were obtained.

© 2016 The Authors. Published by Elsevier Ltd. This is an open access article under the CC BY-NC-ND license (<http://creativecommons.org/licenses/by-nc-nd/4.0/>).

Peer review by the scientific conference committee of SiliconPV 2016 under responsibility of PSE AG.

*Keywords:* copper; screen-printing; silicon solar cell;

---

### 1. Introduction

Improved materials can result in manufacturing silicon-based solar cells at lower cost. The most used method of fabricating front electrodes on the crystalline Si solar cells is screen-printing with the pastes containing Ag powder with additives. This requires sufficiently good contact and therefore good electrical performance of the solar cells. The silver paste contributes to approximately 18% of the total cell production cost, which is appealing for the use of

---

\* Corresponding author. Tel.: +48-122952800; fax: +48-122952804.  
E-mail address: pan-kozy@wp.pl, p.panek@imim.pl

any alternative solution to the silver paste. The replacement of Ag by copper is one of the challenges for the research investigations [1].

In the silicon industry, a copper is considered as a contaminant impurity and it is deleterious to electronic properties of the silicon ingots and wafers [2]. It is necessary to place a buffer layer between Cu and Si in order to prevent a copper diffusion in silicon devices. Additionally, if Ag is used, the buffer thickness has to exceed 20 nm [3]. Other applicable schemes involve formation of Ni silicide with thickness between 30 and 75 nm formed by annealing either electroless or electrolytic deposited Ni [4]. An interesting approach considers a double Ti/TiN layer that led to higher performance of the Si cells as compared to a single Ti layer [5]. Extensive research has been carried out to replace Ag in paste used for screen-printing by less expensive metals such as Ni and Zn, but the results are not promising [1].

Nowadays, a lot of works concerns electroplating of nickel-copper contacts, which offer many advantages and prospects for the metallization of the solar cells [6], but its industrial applications is limited [7]. The usage of Cu paste on electrodes formed by sintering on transparent conductive films at temperature below 200°C was elaborated, but in the case of higher temperature processes, the Cu diffusion issue requires new solutions [8]. A similar approach is to combine screen-printing copper paste deposition with copper fingers formed by light induced plating, but it requires the use of laser ablation to remove the antireflective coating before the plating process [9]. However, the latter method seems industrially inapplicable.

The industrial presently use of Ag in the paste for average screen-printed cell is in the range of 50-120 mg/W. The metal contacts are deposited on the front of the silicon solar cells, following usually a standard H pattern geometry, and on the rear side as 2 or 3 bus-bars [10]. At the end of the printing step, the entire cell assembly is typically co-fired at around 810°C in order to remove the undesired additives used to make the metal pastes. At that temperature, the lead borosilicate glass frit ( $\text{PbO-B}_2\text{O}_3\text{-SiO}_2$ ) formed within the Ag paste etches locally the  $\text{SiN}_x\text{:H}$  layer to form a direct bond and electrical contact with the underlying emitter region [11]. A commercially used pastes contain silver particles, in the form of spherical grains with a mean diameter of 1-2  $\mu\text{m}$ , glass frits, organic binder, and optionally the metallic oxide additives, where the silver amounts to 50-90 wt. % of the mixture. The glass, which usually contains lead oxide (PbO), is less than 5 wt. %, however it plays an important role for the contact formation during the high temperature firing stage. It wets and dissolves silver particles at lowered temperatures, etches and dissolves the anti-reflection coating, and enhances the formation of silver crystallites [12]. The distribution and size of the Ag crystallites formed at the Si emitter interface depends on the PbO content in the glass frit [13]. In case of small Ag particles (with average size of 0.7  $\mu\text{m}$ ), which are sintered in the paste forming a denser contact with the surface that results in lower bulk resistance and better interface structure compared to Ag particle of larger size [14]. Further reduction in the particles diameter to 0.3  $\mu\text{m}$  enhances the electrical conduction and decreases the specific contact resistivity of the paste [15]. The glass can contain other components such as zinc oxide (ZnO) or bismuth oxide ( $\text{Bi}_2\text{O}_3$ ), which depends on the production technology [16]. An example of the composition of the glass frit applied in experimental works is (in wt. %): PbO - 59.30,  $\text{SiO}_2$  - 22.07, ZnO - 8.03,  $\text{Al}_2\text{O}_3$  - 1.14 and  $\text{B}_2\text{O}_3$  - 9.46. Those values clearly demonstrate that lead and silicon oxides play a crucial role [17]. More attention has recently been turned to eliminate heavy metals, such as Pb or Cd, from the solar cell metallization process.

The paper presents investigation concerning newly elaborated composite of CuXX processed copper and commercially available paste used for Si solar cells front electrode deposition by screen-printing method [18].

## 2. Experiment

The CuXX composite was obtained by chemical treatment of copper powder [18]. In this paper, three CuXX components are presented. They differ by weight ratio of XX modifier to the copper grain of 1, 2 and 3 wt. %, which was denoted as CuX1, CuX2 and CuX3, respectively. For the test of applicability, the elaborated paste components were added to commercially available Du Pont PV17D silver paste (CP). The weight ratio of CuXX component to PV17D silver paste was 50%.

The solar cells were fabricated on 1  $\Omega\text{cm}$  p-type Cz-Si (100), 180  $\mu\text{m}$  thick. The cell have a dimension of 5 x 5  $\text{cm}^2$  and a textured surface. The diffusion process was carried out in quartz tube furnace from  $\text{POCl}_3$  donor source at a temperature of 840°C for 30 minutes. The sheet resistance of the final emitter was kept within  $40.1 \pm 1.7 \Omega/\square$ .

The edge isolation was performed in teflon clamp by chemical method, and then the phosphosilicate glass was removed by immersion in a bath of HF: H<sub>2</sub>O (1: 9 vol.) solution for 2 min. The surface passivation was achieved by the growth of 12 nm thick SiO<sub>2</sub> grown at 800°C in dry air for 10 min. To assure an ARC front layer, the 70 nm thick titanium dioxide layer was deposited by CVD method using Ti(C<sub>2</sub>H<sub>5</sub>O)<sub>4</sub> as a source. The screen printing process was carried out with 320 mesh screen and series of pastes PV17D without and with successive addition of CuXX components. PV505 and PV381(Al) pastes were screen-printed on the rear side. After drying in air at 150°C the printed pastes were co-fired in the IR belt furnace running at belt speed of 200 cm/min. The higher real temperature at peak, affecting the Si wafer during metallization process ( $T_{\text{metal}}$ ), was detected by a thermocouple directly clamped to Si. This temperature is significantly lower than a temperature measured by the furnace thermocouple. For this reason, a Datapaq Q19 was used for monitoring the time resolved temperature profiles of products within the metallization process. The IR conveyor furnace applied in an experiment has three heating zones, respectively: 19 cm, 19 cm and 38 cm long, and the temperature during metallization processes has been changed only in the last zone. All processes were performed in a purified and dried natural atmosphere.

The morphology of the copper components and screen printed paths was analyzed by dual beam high-resolution scanning electron microscopy (SEM) FEI Quanta 3D FEG integrated with the EDAX Trident system. A TECNAI G2 F20 - 200 kV FEG transmission electron microscope (TEM) with an energy dispersive spectrum (EDS) detector was used for imaging and composition analysis of the selected part of the front electrode.

The resulting solar cells were characterized by the current-voltage (I-V) measurements thanks to a Solar Simulator SS200 AAA class EM Photo Emission Tech., Inc. with Solar Cells I-V Curve Tracer SS I-V CT-02 PV. The data was obtained under AM1.5 global spectrum at 1000 W/m<sup>2</sup> light intensity at temperature 25°C. The spectral response (SR) properties of the cells were characterized using Jobin Yvon H20 IR monochromator with halogen lamp, working in the wavelength range of 400-1110 nm. The setting up of the beam splitter allowed to simultaneously determinate  $I_{\text{ph}}$  for Hamamatsu photodiode S2281/5D/1299 and  $I_{\text{cell}}$  in the investigated solar cell. The reference cell No. 005-2013 calibrated at Fraunhofer ISE was used in the current-voltage and spectral response measurements. The light beam induced current (LBIC) map was fabricated by a 20 mW diode laser with incident light at 404 nm and spot resolution of about 10 μm.

The X-ray photoelectron spectroscopy (XPS) was used for the analysis of surface composition and electronic states of elements at the contact fingers of the front electrode and at Si n-type emitter surface after finger removing by chemical etching. The measurements were carried out in multifunctional photoelectron spectrometer (RUDI, Prevac) with a hemispherical analyzer (EA14, Prevac, pass energy 100 eV). The Al K $\alpha$  (1486.6 eV) X-ray source was applied to generate core excitations. The surface composition was analyzed with XPS on relatively large area of 3 mm<sup>2</sup>. The analytic depth of the method was c.a. 7 nm. The surface sensitivity of the method for heavy metals was on the level of 0.02 at. %.

### 3. Results and discussion

The SEM imaged morphology of copper powder after chemical processing for CuX3 type of component is shown in Figure 1. The Cu grains are flaky-like in shape and processing does not change their morphology. The CuX3 component shows certain particle agglomeration. Such flaky shape of the particles results in a larger specific surface area and residual stress, causing higher densification of the contact when compared to spherical shape [14].

The CuX3 particles were mixed with commercial Du Pont PV17D silver paste resulting in experimental CP-CuX3 paste presented in Figure 2. The image indicates inhomogeneous distribution of Cu and Ag particles. The inhomogeneity was caused by relatively short time (5 min) mixing procedure. The paste was screen-printed on Si wafer, dried and metallized in IR conveyor furnace. The time resolved temperature profile affecting screen-printed paste on the Si wafer during metallization process is shown in Figure 2b. The effective temperature of the wafer during all experimental works was between 643-798°C.

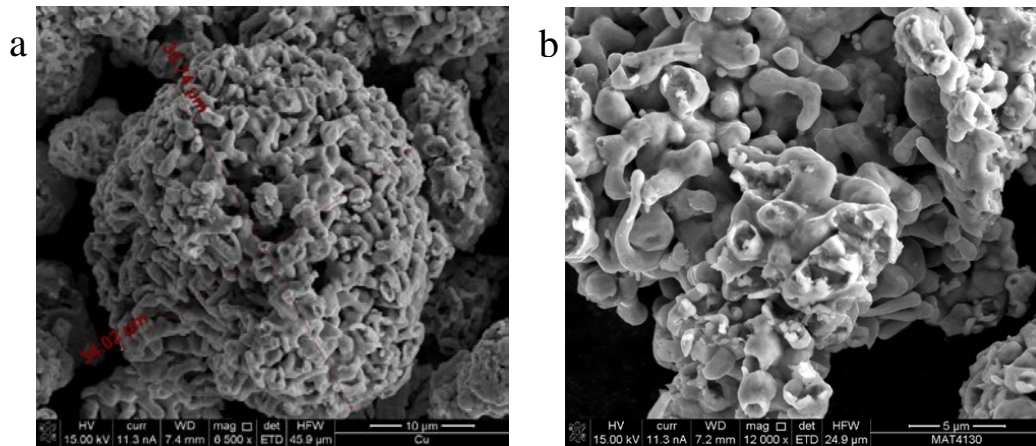


Fig. 1. The SEM images of the processed CuX3 particles.

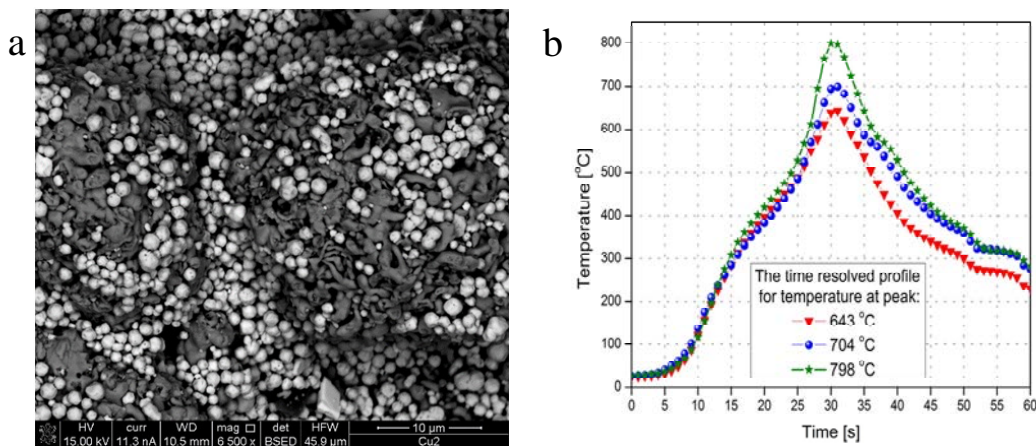


Fig. 2. (a) SEM micrograph presenting mixed CuX3 component and Du Pont PV17D silver paste; (b) The time resolved temperature profiles affecting screen-printed paste on the Si wafer during metallization process in IR furnace.

On the basis of the CuX1 and CuX2 components the solar cells series Cu1 were prepared. The relationship of the fill factor (FF) of the fabricated solar cells and metallization temperature for series Cu1 is shown in Figure 3. The maximum of FF was approached at metallization temperature of 704°C. Direct addition of 50 wt. % of untreated Cu particles into commercial paste PV17D, listed as paste CP-Cu, resulted in a significant FF decrease for temperatures above 720°C. Moreover, the FF value below 50% suggested discontinuation of the work with component based only on untreated Cu grains. The Figure 4 clearly illustrates that the use of chemically treated copper particles (CuX1 and CuX2) allows reaching a FF value above 60%, but still well below the FF value of 75% achievable in the case of PV17D commercial paste application. Based on the results concerning the components CuX1 and CuX2, the component denoted as CuX3 was elaborated as a final product of the experiment.

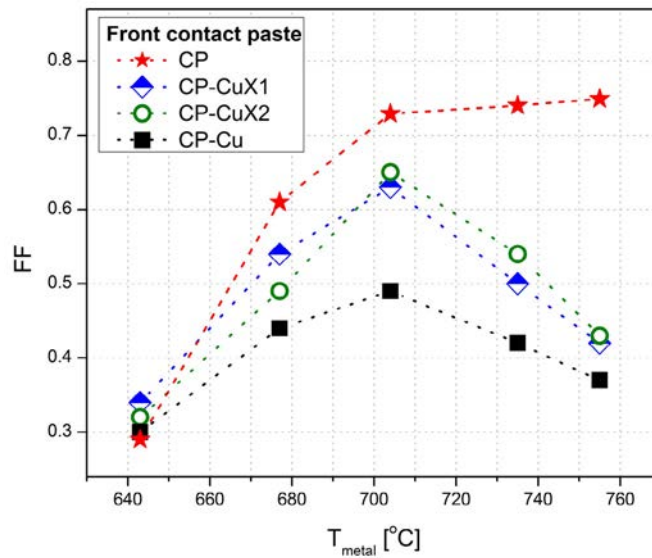


Fig. 3. The dependence of fill factor on metallization temperature for commercial and composite pastes applied for front electrode deposition on the solar cells of Cu1 series.

New paste prepared by mixing of CuX3 component (50 wt. %) with CP paste was prepared and deposited as front electrode by screen-printing method. The fabricated solar cells, signed as series Cu2, were co-fired in the temperature range of 704-798°C and the I-V parameters are summarized in Table 1. For specific temperatures of 755 and 780°C, in which the cells give a value of FF above 70%, the data are collected for the three cells. Table 1 also lists parameters of a reference solar cell (RSC-1), obtained in the same technological process, but with front electrode made only by commercial PV17D paste.

Table 1. The electrical I-V parameters of the 25 cm<sup>2</sup> solar cells with the front contact electrode screen-printed with the mixed CuX3 component and PV17D paste.

Solar Cell	$T_{\text{metal}} [^{\circ}\text{C}]$	$I_{\text{sc}} [\text{A}]$	$V_{\text{oc}} [\text{V}]$	$P_{\text{m}} [\text{W}]$	FF	$R_{\text{s}} [\text{m}\Omega]$	$R_{\text{sh}} [\Omega]$	$E_{\text{ff}} [\%]$
Cu2-1	704	0.742	0.577	0.218	0.509	183.8	6.76	8.73
Cu2-2	712	0.772	0.587	0.283	0.625	146.3	15.71	11.34
Cu2-3	735	0.784	0.593	0.325	0.699	101.1	30.64	12.44
Cu2-4	755	0.811	0.596	0.339	0.702	89.8	54.40	13.58
Cu2-5	755	0.807	0.598	0.348	0.721	86.0	97.22	13.93
Cu2-6	755	0.804	0.594	0.342	0.715	85.1	86.22	13.67
Cu2-7	780	0.805	0.597	0.345	0.717	82.3	54.57	13.80
Cu2-8	780	0.808	0.597	0.341	0.707	83.0	72.94	13.65
Cu2-9	780	0.787	0.596	0.336	0.717	66.2	45.07	13.45
Cu2-10	798	0.815	0.589	0.330	0.687	85.5	62.06	13.20
RSC-1	755	0.801	0.598	0.358	0.750	56.3	108.37	14.35

where:  $T_{\text{metal}}$  – peak temperature,  $I_{\text{sc}}$  – short circuit current,  $V_{\text{oc}}$  – open circuit voltage,  $P_{\text{m}}$  – optimum power point, FF – fill factor,  $R_{\text{s}}$  – series resistance,  $R_{\text{sh}}$  – shunt resistance,  $E_{\text{ff}}$  – conversion efficiency.

The completed fabrication process of the cells with the mixed CuX3 component and PV145 paste resulted in a cell efficiency as high as 13.93% calculated from parameters values:  $V_{oc} = 0.598$  V,  $I_{sc} = 0.807$  A and  $FF = 72.1\%$ . The semi-industrial fabrication system, which was used in the experiment, is not capable to produce cells with conversion efficiency higher than 15-16% [20]. For this reason, the most important parameter opening the possibility of providing effective application for CuX3 component is the fill factor, series and shunt resistance characterizing the produced solar cells. The difference between the cells RSC-1 and Cu2-5 with best conversion efficiency relates to lower shunt and higher series resistances of  $278.7 \Omega\text{cm}^2$  and  $0.732 \Omega\text{cm}^2$ , respectively.

The cell No. Cu2-7 was selected for further studies. The printed paths were imaged by SEM (Fig. 4a). It was found that  $187 \mu\text{m}$  wide and  $21 \mu\text{m}$  thick fingers were printed, leading to rather a low value of the aspect ratio, about 0.11, which should be above 0.25 for high efficiency cells [20].

The light beam induced current (LBIC) map was performed on the previously imaged path (Fig. 4b). In this Figure, blue color represents the highly degraded area of the photoconversion process under the front electrode. At near surface region, the border between contact and textured surface is rather sharp and neither spikes nor defected areas are visible. It suggests that Cu elements are bonded in front finger and the neighbouring emitter region is not contaminated by diffusion of foreign atoms. The distance between borders from the two sides of the finger, shown as red areas in the LBIC map, is about  $180 \mu\text{m}$ , which is appropriate to the finger width determined by SEM.

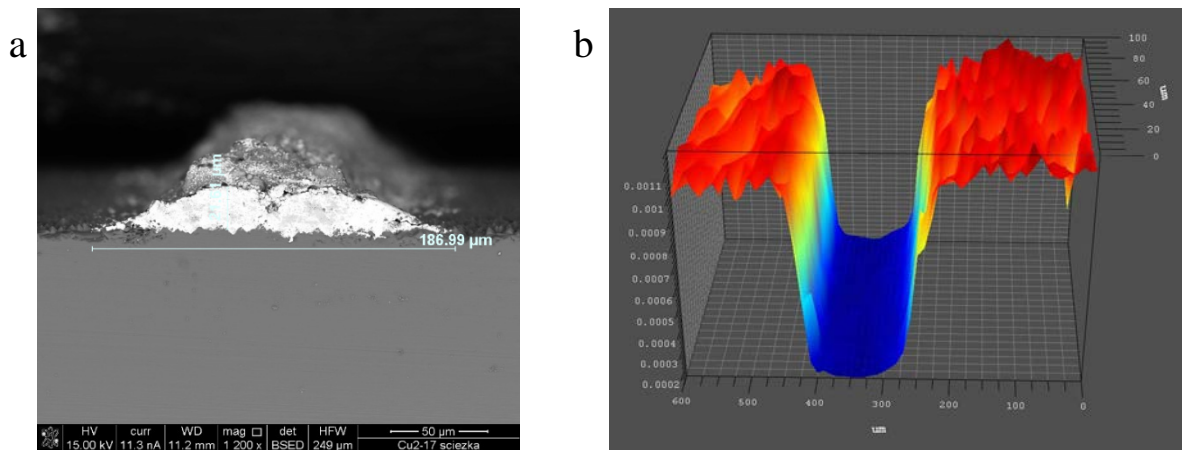


Fig. 4. (a) The SEM micrograph of front finger cross-section; (b) The LBIC map of the electrically degraded area under the front finger.

The measurements of the spectral response (SR) of the cells according to the character of light absorption of a given wavelength in Si were performed in order to evaluate the process of generation and recombination of the charge carriers on the surface of cell (especially in the space charge area). After SR measurements external quantum efficiency (EQE) was calculated and final results are presented in Figure 5.

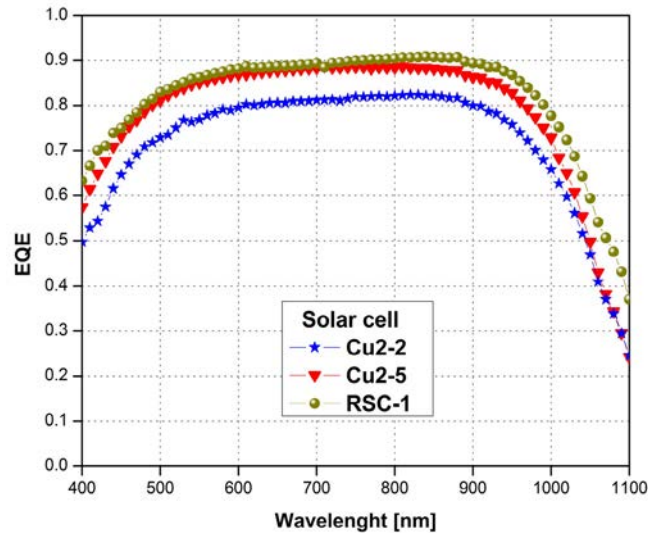


Fig. 5. The EQE curves of Cu2-2, Cu2-5 solar cells fabricated with the mixed CuX3 component and PV17D paste and EQE of the RSC-1 reference cells made with PV17D paste.

The EQE shape is similar for the solar cells obtained for two kind of pastes on the same Si base material and with the same emitter and ARC film. The curves are slightly shifted, which can be explained by difference in  $R_s$  value between that cells (Tab. 1). The quantum efficiency for the cells with electrode formed by the mixed CuX3 component and PV17D paste does not show the degradation effect, especially concerning photoconversion process in short wavelength region between 400 and 500 nm, which is a very promising result that suggests a lack of Cu impurity under the electrode i.e. in the emitter region.

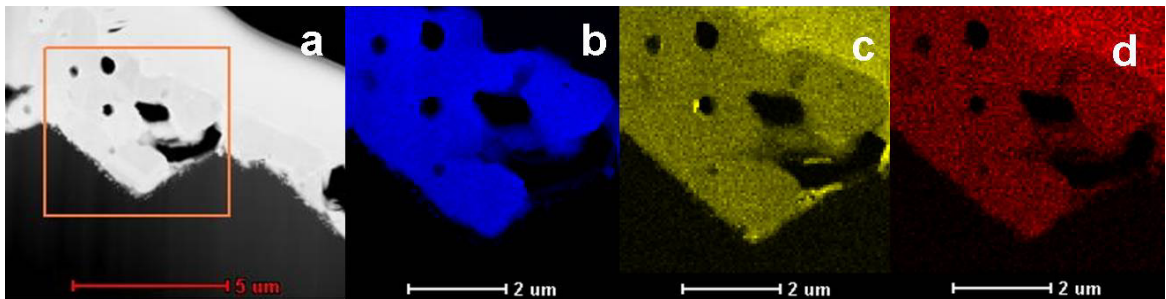


Fig. 6. (a) TEM image of the screen printed path and the respective element distribution maps of (b) Ag; (c) Cu and (d) X3 modifier.

In order to observe distribution of metallic components on the path surface, TEM microscope presents the maps of element distribution on the screen printed path (Fig. 6). Figures 6b-d exhibits an homogenous distribution of Cu, Ag and the element X3 used for copper grains modification. The TEM image shows also empty spaces in the bulk material of a front contact, which are obviously created during the screen-printing process and contributed to the higher series resistance of the solar cells Cu2 series. The spaces can be caused by lower proportion of the organic carriers in the paste due to mixing of CuXX component at rather high ratio of 50 wt. %. As a second factor, the mixing procedure should be extended over 5 min. (Fig. 2a). Moreover, the resulting paste CP-CuX3 shows higher viscosity than the original PV17D paste and consequently disturbs the quality of screen-printing deposition.

The lower fill factor of the Cu2 cells relates to lower series resistance, caused by a change of physical parameters of the PV17D paste. This resulted in the low aspect ratio (Fig. 4a) and empty spaces in front finger massive material

(Fig. 6). The results provide the foundation and justification for research aimed at optimizing the new paste with CuXX component taking into account the influence of paste rheology and screen-printing process parameters on the front side metallization of the silicon solar cell [20].

The XPS was used for the analysis of surface composition on the front electrode and under the electrode. For this investigation, the cell No. Cu2-7 was chosen. The central bus bar was analyzed prior and after etching in  $\text{HCl} : \text{HNO}_3 : \text{H}_2\text{O}$  (10:1:9 vol.) solution for 10 min. at temperature of  $45^\circ\text{C}$ . The etching was applied to remove the body of the copper-containing path.

Analysis of the XP spectra (Fig. 7) revealed that the investigated surfaces differ qualitatively only by copper that is absent at the etched surface. The common elements for both surfaces are Si, O, Ag, Ti. The existence of Ti in the emitter region after etching can be explained by the fact that  $\text{TiO}_2$  is deposited on Si cell surface as an antireflective coating. The high resolution Cu 2p spectra (Fig. 7b) were also acquired prior and after etching. The Cu 2p spectrum showed broadened doublet followed by shake-up satellites. The broadening of the core excitations suggested presence of metallic and oxide copper compounds and intensity of satellites indicated that only part of metallic copper is oxidized [21]. The path etching resulted in total removal of copper from the surface whereas silver has been still present at the etched surface. These outcomes indicate that copper does not contaminate the path/silicon interface and it fills only the path's body.

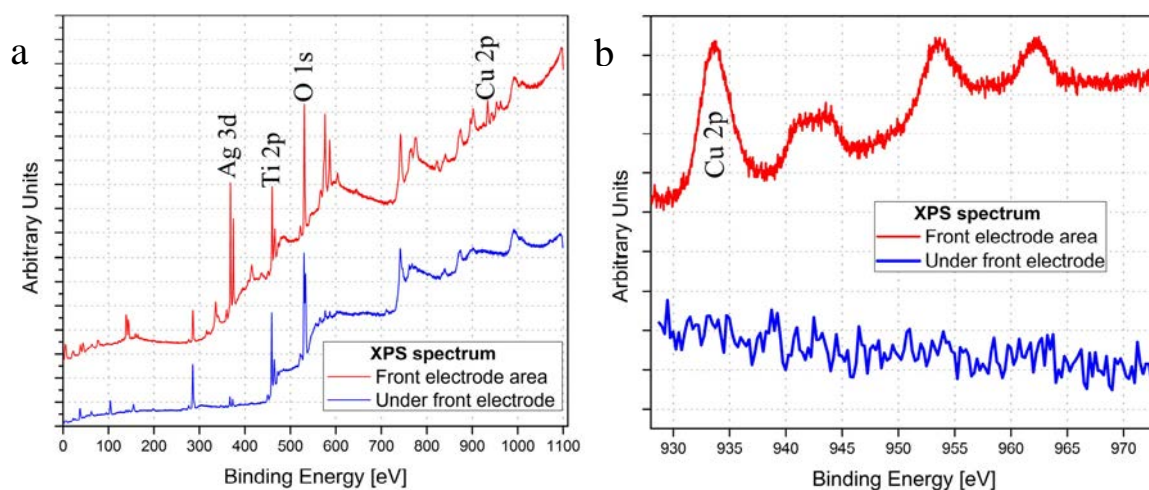


Fig. 7. (a) The XP survey and (b) high resolution Cu 2p spectra of the front electrode of Cu2-7 cell prior (red, top) and after (blue, bottom) etching.

#### 4. Conclusions

The paper presents the CuXX copper-based component that can partly substitute silver in the pastes used for screen-printing of the electrical paths in silicon solar cells. Mixing with commercial paste tested the use of CuXX component. The obtained solar cells showed opto-electrical parameters comparable to the ones obtained with pure commercial paste. Despite the non-optimized technology process, the fill factor of 0.72 was achieved. Additionally, after one year of experimental testing, no degradation of parameters of the Cu2 series solar cells has been observed. The research results lead to the conclusion that the paste with Cu can be used for solar cells produced in high-temperature processes. Therefore, the results provide an important foundation for further research aimed on optimization of the CuXX component and parameters concerning mixed systems.

## Acknowledgements

This work has been carried out in the frame of IMMS statutory activity.

## References

- [1] Rudolph D, Olibet S, Hoornstra J, Weeber A, Cabrera E, Carr A, Koppes M, Kopecek R. Replacement of silver in silicon solar cell metallization pastes containing a highly reactive glass frit: Is it possible? *Energy Procedia* 2013;43:44-53.
- [2] Gaspar G, Modanese C, Schøn H, Sabatino MD, Arnberg L, Øvrelid EJ. Influence of copper diffusion on lifetime degradation in n-type Czochralski silicon for solar cells. *Energy Procedia* 2015;77:586-91.
- [3] Yukawa M, Kitagawa H, Lida S. Effect of an Ag buffer layer on Cu/Ag/Si system. *Applied Surface Science* 2004;237:156-60.
- [4] Huang Q, Reuter KB, Zhu Y, Deline VR. A study of the long-term degradation of crystalline silicon solar cells metallized with Cu electroplating. *ECS Journal of Solid State Science and Technology* 2016;5:Q24-34.
- [5] You JS, Kang J, Kim D, Pak JJ, Kang CS. Copper metallization for crystalline Si solar cells. *Solar Energy Materials & Solar Cells* 2003;79:339-45.
- [6] Bartsch J, Brand A, Eberlein D, Mondon A, Völker C, Tranitz M, Graf M, Nekarda J, Eitner U, Philipp D, Glatthaar M. Simple and reliable process for creating fully plated nickel-copper contacts. *Photovoltaics International* 2014;3:49-57.
- [7] Rehman ur A, Lee SH. Review of the potential of the Ni/Cu plating technique for crystalline silicon solar cells. *Materials* 2014;7:1318-41.
- [8] Yoshida M, Tokuhisa H, Itoh U, Kamata T, Sumita I, Sekine S. Novel low temperature-sintering type Cu-alloy pastes for silicon solar cells. *Energy Procedia* 2012;21:66-74.
- [9] Wood D, Kuźma-Filipek I, Russel R, Duerinckx F, Powell N, Zambova A, Chislea B, Chevalier P, Boulord C, Beucher A, Zeghers N, Szlufcik J, Beaucarne G. Non-Contacting busbars for advanced cell structures using low temperature copper paste. *Energy Procedia* 2015;67:101-7.
- [10] Green MA. Ag requirements for silicon wafer-based solar cells. *Progress in Photovoltaics: Research and Application* 2011;19:911-6.
- [11] Goodrich A, Hacke P, Wang Q, Sopori B, Margolis R, James TL, Woodhouse M. A wafer-based monocrystalline silicon photovoltaics road map: Utilizing known technology improvement opportunities for further reductions in manufacturing costs. *Solar Energy Materials & Solar Cells* 2013;114:110-35.
- [12] Kalio A, Leibinger M, Filipovic A, Krüger K, Glatthaar M, Wilde J. Development of lead-free silver ink for front contact metallization. *Solar Energy Materials & Solar Cells* 2012;106:51-4.
- [13] Hong KK, Cho SB, You JS, Jeong JW, Bea SM, Huh JY. Mechanism for the formation of Ag crystallites in the Ag thick-film contacts of crystalline Si solar cells. *Solar Energy Materials & Solar Cells* 2009;93:898-904.
- [14] Zhou J, Xu N, Yang H, Zhang Q. Effect of Ag powder and glass frit in Ag paste on front contact of silicon solar cells. *Procedia Engineering* 2014;94:1-5.
- [15] Li W, Wu T, Jiao R, Zhang BP, Li S, Zhou Y, Li L. Effects of silver nanoparticles on the firing behavior of silver paste on crystalline silicon solar cells. *Colloids and Surfaces A: Physicochem Eng Aspects* 2015;466:132-7.
- [16] Hoenig R, Kalio A, Sigwarth J, Clement F, Glatthaar M, Wilde J, Biro D. Impact of screen printing silver paste components on the space charge region recombination losses of industrial silicon solar cells. *Solar Energy Materials & Solar Cells* 2012;106:7-10.
- [17] Cho SB, Hong KK, Huh JY, Park HJ, Jeong JW. Role of the ambient oxygen on the silver thick-film contact formation of crystalline silicon solar cells. *Current Applied Physics* 2010;10:S222-5.
- [18] Panek P, Socha PR, Drabczyk K. The component of a conductive paste and conductive paste especially for solar cells electrode deposition. Polish Patent Office, Warsaw, 2014, No P.409794.
- [19] Panek P, Drabczyk K, Zięba P. Crystalline silicon solar cells with high resistivity emitter. *Opto-Electronics Review* 2009;17:161-5.
- [20] Thibert S, Jourdan J, Bechevet B, Chaussy D, Reverdy-Bruas N, Beneventi D. Influence of silver paste rheology and screen parameters on the front side metallization of silicon solar cell. *Materials Science in Semiconductor Processing* 2014;27:790-9.
- [21] Dźwigaj S, Janas J, Gurgul J, Socha RP, Shishido T, Che M. Do Cu(II) ions need Al atoms in their environment to make CuSiBEA active in the SCR of NO by ethanol or propane? A spectroscopy and catalysis study. *Appl. Catal. B: Environmental* 2009;85:131-8.